Published in final edited form as:
Exp Cell Res. 2010 October 15; 316(17): 2859–2870. doi:10.1016/j.yexcr.2010.06.014.

MIST1 Regulates the Pancreatic Acinar Cell Expression of *Atp2c2*, the gene encoding Secretory Pathway Calcium ATPase 2

Victoria C. Garside[1,2,3], **Agnes S. Kowalik**[1,2,4], **Charis L. Johnson**[1,2,4], **Daniel DiRenzo**[5], **Stephen F. Konieczny**[5], and **Christopher L. Pin**[1,2,4]

Stephen F. Konieczny: sfk@purdue.edu; Christopher L. Pin: cpin@uwo.ca

[1]Children's Health Research Institute, London, Ontario

[2]Department of Paediatrics, The University of Western Ontario, 800 Commissioners Rd E, London Health Sceinces Centre, London, Ontario, CANADA, N6C 2V5

[3]Department of Biology, The University of Western Ontario, 800 Commissioners Rd E, London Health Sceinces Centre, London, Ontario, CANADA, N6C 2V5

[4]Department of Physiology & Pharmacology, The University of Western Ontario, 800 Commissioners Rd E, London Health Sceinces Centre, London, Ontario, CANADA, N6C 2V5

[5]Department of Biological Sciences and the Purdue Center for Cancer Research, Purdue University, Hansen Life Sciences Research Building, 201 South University Street, West Lafayette, IN, USA 47907-2064

Abstract

MIST1 is a transcription factor expressed in pancreatic acinar cells and other serous exocrine cells. Mice harboring a targeted deletion of the *Mist1* gene (*Mist1*$^{-/-}$) exhibit alterations in acinar regulated exocytosis and aberrant Ca^{2+} signaling that are normally controlled by acinar cell Ca^{2+}-ATPases. Previous studies indicated that total sarcoendoplasmic reticulum Ca^{2+}-ATPases (SERCA) and plasma membrane Ca^{2+}-ATPases (PMCA) remained unaffected in *Mist1*$^{-/-}$ acinar cultures. Therefore, we have assessed the expression of *Atp2c2*, the gene that encodes the secretory pathway Ca^{2+}-ATPase 2 (SPCA2). We revealed a dramatic decrease in pancreatic expression of *Atp2a2* mRNA and SPCA2 protein in *Mist1*$^{-/-}$ mice. Surprisingly, this analysis indicated that the acinar-specific *Atp2c2* mRNA is a novel transcript, consisting of only the 3′ end of the gene and the protein and localizes to the endoplasmic reticulum. Expression of SPCA2 was also lost in *Mist1*$^{-/-}$ secretory cells of the salivary glands and seminal vesicles, suggesting that *Atp2c2* transcription is regulated by MIST1. Indeed, inducible MIST1 expression in *Mist1*$^{-/-}$ pancreatic acinar cells restored normal *Atp2c2* expression, supporting a role for MIST1 in regulating the *Atp2c2* gene. Based on these results, we have identified a new *Atp2c2* transcript, the loss of which may be linked to the *Mist1*$^{-/-}$ phenotype.

Keywords

bHLH transcription factors; Ca^{2+} ATPases; Golgi apparatus; pancreatic acinar cells; regulated exocytosis; bHLHa15

Corresponding Author: Dr. Christopher Pin, Dept. of Paediatrics, The University of Western Ontario, Children's Health Research Institute, 5th Floor, Victoria Research Laboratories, London, Ontario, Canada, N6C 2V5, Phone: (519) 685-8500, ext. 53073, FAX: (519) 685-8186, cpin@uwo.ca.
Current address: Victoria C. Garside, Terry Fox Laboratory, BC Cancer Agency, Vancouver, British Columbia, University of British Columbia, Department of Cell and Development, Vancouver, British Columbia.

Introduction

MIST1 is a transcription factor belonging to the class B family of basic helix-loop-helix (bHLH) proteins [1]. Class B bHLH proteins typically exhibit tissue specific expression and affect transcription of genes involved in cell determination, differentiation and cellular functions. *Mist1* (also referred to as *Basic helix loop helix a15; Bhlha15,* or *dimmed* in *Drosophila*) is expressed in all serous type exocrine cells including pancreatic and salivary acini, Chief cells of the stomach, and secretory cells of the seminal vesicle, prostate and lactating mammary gland [2]. All MIST1 expressing cells rely on regulated exocytosis for their primary function. During regulated exocytosis, Ca^{2+} is tightly controlled with release into and uptake from the cytosol being regulated by proteins that act as ion channels and pumps, respectively [3, 4]. Upon secretagogue stimulation, *Mist1*$^{-/-}$ pancreatic acini exhibit a rapid release of Ca^{2+} into the cytosol but clearance of Ca^{2+} from the cytosol does not occur, leading to sustained high levels of cytosolic Ca^{2+} within *Mist1*$^{-/-}$ acinar cells [5]. The defective Ca^{2+} signaling in *Mist1*$^{-/-}$ acinar cells suggests that expression of proteins regulating Ca^{2+} movement within the cell may be compromised.

The key protein families involved in maintaining appropriate levels of cytosolic Ca^{2+} are the Ca^{2+}-ATPases. Ca^{2+}-ATPases belong to the phosphorylation-type (P-type) ATPase family and include sarcoendoplasmic reticulum Ca^{2+}-ATPases (SERCAs), plasma membrane Ca^{2+}-ATPases (PMCAs) and secretory pathway Ca^{2+}-ATPases (SPCAs) [6–8]. These pumps either move activator Ca^{2+} out of the cell (PMCAs) or move Ca^{2+} from the cytosol back into Ca^{2+} stores such as the ER (SERCAs) and Golgi (SPCAs) [9]. Previous studies indicated no change in the total expression levels of SERCA and PMCA proteins in *Mist1*$^{-/-}$ acini cultures but the SPCA proteins were not examined [5].

In this study, we examined expression of the *Atp2a, -b, -c* gene family in wild type (WT) and *Mist1*$^{-/-}$ mice. In *Mist1*$^{-/-}$ pancreata, expression of *Atp2c2*, correlating to the SPCA2 protein, was dramatically decreased relative to WT tissue. A similar decrease was observed in all tissues examined that normally express MIST1. Loss of SPCA2 correlated with expansion of the Golgi compartment and disruption of Golgi function. Re-establishment of MIST1 expression in *Mist1*$^{-/-}$ pancreata resulted in restoration of *Atp2c2* transcript levels. These results suggest that *Atp2c2* is a downstream target of MIST1 transcriptional activity and may be responsible, in part, for defective Ca^{2+} signaling in *Mist1*$^{-/-}$ pancreata.

Experimental Procedures

All chemicals were purchased from Sigma (St. Louis, MO) unless otherwise stated.

Mice

C57 Bl/6 mice were handled according to the regulations set for The University of Western Ontario Animal Care by the Canadian Council of Animal Care (protocol #2008-116). Mice lacking *Mist1* (*Mist1*$^{-/-}$) have been previously described [10]. Transgenic mice (*LSL-Mist1*^{myc}) were generated that express a myc-tagged MIST1 protein that can be selectively activated through Cre-mediated recombination. Mice harboring a targeted replacement of the *Mist1* gene with CreER^{T2} (*Mist1*$^{CreER/CreER}$) have been previously described [11]. Standard crosses were performed to produce a *Mist1*$^{-/-}$ mouse containing the CreER^{T2}-inducible LSL-*Mist1*^{myc} transgene (*LSL-Mist1*^{myc}/*Mist1*$^{CreER/CreER}$). Induction of *Mist1*^{CreER} activity was accomplished by providing 8 week *Mist1*$^{CreER/CreER}$/*LSL-Mist1*^{myc} mice (in triplicate for each group and time point) a single dose of tamoxifen (4 mg/mouse) or control corn oil as previously described [11]. All mice were provided with a standard diet and water *ad libidum*.

RNA isolation and quantification

All reagents were from Promega (Ottawa, ON) unless otherwise stated. RNA was isolated from the pancreas as described [12] or from whole tissues, primary acinar cell cultures, or AR42J and ARIP cell lines using Trizol (Invitrogen, Burlington, ON) as per manufacturer's protocol. Alternatively, pancreas RNA was isolated at 24 hr, 48 hr, and 72 hr post-tamoxifen treatment of *Mist1*$^{CreER/CreER}$/*LSL-Mist1*^{myc} mice using the RNeasy isolation system (QIAGEN, Valencia, CA) and reverse transcribed using the iScript^{TM} cDNA synthesis kit (Bio-Rad, Hercules, CA). For RT-PCR, 1 μg of total RNA was reversed transcribed using random primers and Improm II reverse transcriptase, then amplified through 35 rounds of denaturing (94°C for 30 s), annealing (60–68°C for 40 s), and elongation (72°C for 60 s). For primer sequences and conditions see Table S1. All primers were designed using sequences from the National Center for Biotechnology Information web database (www.ncbi.nlm.nih.gov) and generated by Sigma-Genosys (Oakville, ON).

Quantitative (q) RT-PCR was performed using the Roche LightCycler® 2.0 System (Roche, Mannheim, Germany) with the LightCycler® FastStart DNA Master^{PLUS} SYBR Green I kit. The amplification process consisted of an initial denaturation step (95°C for 10 s), a reaction cycle (95°C for 10 s), annealing (59.9–68.1°C for 5 s), and elongation (72°C for 10 s). For primer sequences and conditions see Table S1.

Northern blot analysis was performed as described [12]. Blots were hybridized overnight at 42°C with α^{32}P-dCTP-radiolabeled probe (1×10^6 cpm/ml). The template for the probe was made from DNA plasmids containing the *Atp2c2* sequence.

SPCA2 antibody generation and protein analysis

In collaboration with ProSci Inc. (Poway, CA), a peptide sequence for antibody production was determined using the sequence of the carboxy-terminal domain of the mouse SPCA2 (NCBI Accession #ABS18966). The optimal antigenic site was determined to be KLWEKFLSRARPTQMLPEAV.

Protein was isolated and western blot analysis was performed as described [13]. 10–50 μg of protein was resolved by SDS-PAGE and transferred to PVDF membrane (BioRad, Hercules, CA). The rabbit anti-SPCA2 (1:3000) and anti-β-tubulin (1:500, Santa Cruz) were recognized by HRP-conjugated goat anti-rabbit IgG (1:10000; Jackson Immunoresearch Labs, West Grove, PA). The mouse anti-adaptin γ and anti-GM130 (1:500, 1:1000, respectively, BD Biosciences, Mississauga, ON) were recognized by HRP-conjugated goat anti-mouse IgG (1:2000, Jackson Immunoresearch Labs). As a control for the specificity of the SPCA2 antibody, western blots were repeated using preimmune serum or following preabsorption with purified SPCA2 antigen.

For immunohistochemistry (IHC), pancreatic tissue was isolated from WT and *Mist1*$^{-/-}$ mice, embedded in paraffin and sectioned to 5 μm. Following deparaffinization, antigen retrieval was performed with a 20 minute incubation in sodium citrate buffer (pH=6) followed by washing in PBS, 2 × 5 minute washes with 0.2% Triton X in PBS, and more washes in PBS. Endogenous HRP activity was quenched with a 5 minute incubation in 3% H_2O_2. Sections were blocked for 30 minutes in 10% goat serum and incubated for one hour at room temperature in primary antibodies diluted in blocking serum. Following PBS washes, sections were incubated in biotinylated secondary antibodies diluted in blocking serum for 30 minutes at room temperature, washed and then incubated for 30 minutes at room temperature in ABC complex, prepared as described by manufacturer (Pierce, Rockford, IL). HRP was detected with a diaminobenzidine staining kit (Pierce, Rockford, IL) and then sections were washed counterstained with hematoxylin. For immunofluorescence (IF), pancreata were processed as described [10].

Primary antibodies used included rabbit anti-SPCA2 (1:250), rabbit anti-calreticulin (1:250; Chemicon), mouse anti-GM130 (1:200, BD Biosciences), mouse anti-SERCA2 (Pierce, Rockford, IL) and mouse anti-adaptin γ (1:250, BD Biosciences). Secondary antibodies included biotinylated goat-anti mouse IgG or anti rabbit IgG (1:200), fluorescein isothiocyanate (FITC) goat anti-rabbit IgG and tetramethylrhodamine isothiocyanate (TRITC) goat anti-mouse IgG (1:250; Jackson Immunoresearch Labs, West Grove, PA). In some cases, IF was combined with FITC-conjugated wheat germ agglutinin (WGA; incubated 1:1000). IF was visualized with a Leica DMIOS upright microscope or an Olympus Fluoview FV1000 confocal microscope. Images were captured using the Open Lab 3.1.5 imaging program (Quorom Techniologies, Guelph, ON) or FV 10-ASW 1.6 (FluoView 1000 software, Olympus corporation) and Image-Pro Analyzer (version 6.2, Media Cybernetics) software, respectively.

In situ hybridization

In situ hybridization was performed on 7 μm cryosections as described [13]. Digoxigenin-labelled RNA probes were synthesized by *in vitro* transcription of region-spanning parts of the *insulin* and *amylase* coding regions from pancreatic cDNA and the *Atp2c2* clone (#4984604) (for primer sequences, see Table S1) using T3 RNA polymerase. Staining was visualized using OpenLab 4.0.3 Modular Software for Scientific Imaging.

Construct design and cloning

To generate FLAG-tagged, C-terminal SPCA2 expression vector, primers were designed to amplify exons 24 to 27 of the *Atp2c2* gene (Table S1). FLAG-*Spca2*$^{760\text{-}944}$ was amplified from *pCMV-SPORT6-3′Spca2* plasmid (clone # 4984604) and ligated into the *pSC-A* vector using the Strataclone™ PCR Cloning kit (Stratagene, La Jolla, CA). *pSC-A-FLAG-Spca2*$^{760\text{-}944}$ was digested with *XbaI* and *BamHI* and ligated into *pcDNA3.0(+)* (cut with the same enzymes) using the Roche Rapid DNA ligation kit and transformed into DH5α *E. coli* competent cells (Invitrogen).

Cell culture and transfection

All cell culture reagents were purchased from Gibco (Burlington, ON) unless otherwise stated. Primary cell cultures were established as described [14]. ARIP and AR42J were maintained in F12 Kaighn's Modification (F12-K) media containing 4 mM L-glutamine, 1% Pencillin/Streptomycin (Penstrep) and 10% (ARIP) or 20% (AR42J) fetal bovine serum (FBS). HEK 293T (ATCC, Manassas, VA) were maintained in 1X Dulbecco's Modified Eagle Medium (DMEM) high glucose media containing 4.5 g/L D-glucose, 4 mM L-glutamine, 10% FBS and 1% Penstrep. Transfections of HEK 293T cells were performed at 50–60% confluency in 6-well plates with *pcDNA3.0-FLAG-SPCA2*$^{760\text{-}944}$, *pcDNA3-Mist1*^{HA} and *pcDNA3-GFP* constructs. A total of 1 μg of DNA was added per well in 1X HEPES Buffered Saline Solution (HBSS) and 125 mM $CaCl_2$. The solution was gently agitated and added to each well in a dropwise manner. Media was changed the following day and protein isolated or cells were fixed for IF 48 hours after transfection.

Results

Loss of MIST1 results in altered Ca^{2+} movement and decreased regulated exocytosis in pancreatic acinar cells [5] (Supplemental Figure S1). Analysis of individual proteins involved in Ca^{2+} movement within the cell revealed a decrease in IP_3R3 accumulation but no change in the protein levels of the SERCA or PMCA pumps in isolated acini [5, 15]. The maintained expression of the SERCA and PMCA pumps was surprising since *Mist1*$^{-/-}$ acinar cells exhibit severe defects in moving Ca^{2+} back out of the cytosol following secretagogue stimulation. To address this issue, we examined expression of the *Atp2* gene

family in WT and *Mist1*$^{-/-}$ pancreatic tissue from 2- and 12-month old mice. As shown in Figure 1A, a marked increase in expression of many *Atp2* genes was observed in *Mist1*$^{-/-}$ tissues, suggesting that *Mist1*$^{-/-}$ acinar cells attempt to compensate the increased cytosolic Ca^{2+} pools by increasing *Atp2* levels within the cell. Indeed, increased cytosolic Ca^{2+} has been shown to increase expression of several Ca^{2+}-ATPases in other models [16, 17], so a compensatory increase in the SERCA and PMCA pumps would not be surprising. The only exception to the compensation mechanism was the *Atp2c2* gene where transcripts were readily detected in all WT pancreatic samples but were absent in *Mist1*$^{-/-}$ pancreata (Figure 1A). The decrease in *Atp2c2* expression was confirmed by qRT-PCR (Figure 1B), Northern blot (Figure 1C) and *in situ* hybridization analyses (Figure 1D–I) where *Atp2c2* transcripts were exclusively restricted to acinar cells (Figure 1D).

To further examine SPCA2, which is the protein encoded by the *Atp2c2* gene, we generated an antibody specific for its C-terminal region. Western blots of protein extracts from HEK 293T cells transfected with expression vectors for a truncated FLAG-tagged SPCA2 (*FLAG-SPCA2*$^{760\text{-}944}$), HA-tagged MIST1 or control GFP protein identified the expected 20 kDa band corresponding to the truncated FLAG-SPCA2$^{760\text{-}944}$ protein (Figure 2A). Similarly, the SPCA2 antibody recognized a protein in the acinar cell line AR42J, but not in ARIP cells which are MIST1 negative [2]. Surprisingly, the protein size in AR42J cells was only slightly larger than the truncated *FLAG-SPCA2*$^{760\text{-}944}$ protein. This protein was not observed following Western blot analysis after preabsorption with a SPCA2 blocking peptide or with preimmune serum (Supplemental Figure S2). The lower molecular weight isoform of SPCA2 was detected in whole pancreatic and brain protein samples (Figure 2B) but not in *Mist1*$^{-/-}$ protein extracts (Figure 2C), suggesting that SPAC2 in pancreatic cells is much smaller than its NCBI-predicted molecular mass. Again, preabsorption with the SPCA2 blocking peptide completely abolished detection of the 20 kDa protein even with extended exposures (Figure 2C). Interestingly, we did not detect the published full-length (103 kDa) SPCA2 protein in pancreatic extracts, although this larger isoform was detected in brain samples (Figure 2B).

In an effort to establish if the smaller pancreas SPCA2 protein was the product of degradation, we assessed the size of *Atp2c2* transcripts. Northern blot analysis revealed that the pancreas produced a much smaller *Atp2c2* transcript than the expected full length transcript (Figure 1C). Quantitative RT-PCR confirmed that transcripts encoding exons 24–27 were approximately 100-fold more abundant in pancreas and 5-fold more abundant in salivary gland samples when compared to transcripts encoding exons 15–17 (Supplemental Figure S3). Importantly, this difference in amplification was not observed in RNA samples from testes, where both sets of primers amplified equivalent amounts of *Atp2c2* transcripts. Together, these data suggest that an alternative size transcript of *Atp2c2* exists in the pancreas whose expression is regulated by MIST1.

To date, no targeted knockout of *Atp2c2* has been reported. However, ablation of the closely related *Atp2c1* gene resulted in expansion of the Golgi complex and an altered ER stress response [18]. Previous studies from our group showed that *Mist1*$^{-/-}$ acini also exhibit an altered ER stress response [12], suggesting that pancreatic SPCA2 may play a similar role as SPCA1. To address this, we next examined the overall organization of acinar Golgi in WT and *Mist1*$^{-/-}$ pancreata using cis (GM130) and trans (adaptin γ) Golgi-specific markers. Confocal immunofluorescence (IF) analysis revealed an expansion of the Golgi complexes in *Mist1*$^{-/-}$ acini (Figure 3A–D). Western blots confirmed an increase in adaptin γ and GM130 proteins in *Mist1*$^{-/-}$ tissue (Figure 3E). To determine if Golgi function was disrupted in acinar cells lacking MIST1, WT and *Mist1*$^{-/-}$ pancreas sections were incubated with a FITC-conjugated wheat germ agglutinin (WGA), which recognizes sialic acid and N-acetylglucosaminyl sugar residues on glycosylated proteins that are processed through the

Golgi. Fluorescent imaging revealed a marked decrease in lectin accumulation in *Mist1*$^{-/-}$ acinar cells compared to WT pancreata (Figures 4 and S4). FITC-WGA primarily detects acinar cell zymogen granules and does not co-localize with the endoplasmic reticulum (Figure 4). The decrease in FITC-WGA binding in *Mist1*$^{-/-}$ samples supports the idea of improper Golgi function in *Mist1*$^{-/-}$ acinar cells and this alteration correlates with the absence of SPCA2. Interestingly, *Mist1*$^{-/-}$ pancreata also have decreased calreticulin accumulation (Figure 4A, D, G), suggesting widespread defects in the Golgi and ER compartments of these cells.

To assess the location of SPCA2 accumulation in the pancreas, IHC analysis was performed on paraffin sections (Figure 5). Expression was observed throughout acinar tissue (Figure 5A) and in a subset of islet cells (Figure 5B) typically restricted to cells at the periphery of the islets. Pancreatic ducts (Figure 5A), intercalated ducts (Figure 5C) and blood vessels (Figure 5D) were all negative for SPCA2 accumulation. Interestingly, the loss of SPCA2 in *Mist1*$^{-/-}$ tissue is specific to acinar cells as SPCA2+ islet cells are still observed in the islets of *Mist1*$^{-/-}$ pancreata (Figure 5F). These cells are not β cells as they did not stain for insulin expression based on co-IF analysis (Figure 5G, H). Surprisingly, the majority of SPCA2 appeared to accumulate in the basolateral region of pancreatic acinar cells (Figure 5), consistent with localization to the ER. To assess intra-acinar localization (Figure 6), SPCA2 accumulation was compared to markers for the Golgi apparatus (adaptin γ) and ER (calreticulin and SERCA2). Pancreatic acinar cells have a highly organized intracellular structure with the Golgi apparatus positioned between the basally-localized nuclei and the apical-located zymogen granules [19]. SPCA2 accumulation (Figure 6A) was consistent with calreticulin (Figure 6D) and SERCA2 (Figure 6E) localization, limited to the basal portion of the acinus. Adaptin γ (Figure 6C) accumulated just apical to the ER. To verify that pancreas SPCA2 does not localize to the Golgi, we next performed co-IF using antibodies against SPCA2 and either GM130 or adaptin γ (Figure 7). In confirmation of the IHC results, SPCA2 did not co-localize with GM130 (Figure 7A,C,E) or adaptin γ (Figure 7B,D,F) in the Golgi, but instead remained associated with the basal aspect of the cell.

The absence of SPCA2 in *Mist1*$^{-/-}$ pancreatic tissue suggests that the *Atp2c2* gene is a downstream transcriptional target of MIST1. Consistent with a role for MIST1 in the regulation of *Atp2c2* expression, other tissues that normally express MIST1, including the salivary glands and seminal vesicle, also showed a decreased level of *Atp2c2* transcripts in *Mist1*$^{-/-}$ tissues (Figure 8A). In contrast, *Atp2c2* gene expression was similar in WT and *Mist1*$^{-/-}$ testes, a tissue that does not express MIST1. IF localization confirmed that *Mist1*$^{-/-}$ salivary glands (Figure 8B–C) and gastric glands of the stomach (Figure 8D–I), exhibited a dramatic reduction in SPCA2 levels. Importantly, SPCA2 levels were not altered in the surface epithelial cells of the stomach (arrowheads in Figure 8D, E), which never express MIST1.

To support *Atp2c2* as a downstream target of MIST1, we employed a genetic mouse model in which expression of a MIST1 transgene (*LSL-Mist1*^{myc}) can be selectively activated through Cre-mediated recombination (unpublished data). *LSL-Mist1*^{myc}*/Mist1*$^{CreER/CreER}$ (*Mist1*$^{-/-}$) mice were then generated through standard crosses producing a *Mist1*$^{-/-}$ mouse containing a *CreER*^{T2}-inducible transgene. As shown in Figure 7, *Atp2c2* transcripts were virtually undetectable in *Mist1*$^{-/-}$ pancreata. However, 24 hr following a single dose of tamoxifen, MIST1^{myc} expression was induced in ~85% of acinar cells (data not shown) and this led to a 37% increase in endogenous *Atp2c2* transcript levels, which continued to increase to WT levels over the next two days (Figure 9). Thus, *Atp2c2* gene expression was completely restored in *Mist1*$^{-/-}$ acinar cells upon *Mist1*^{myc} transgene expression, strongly suggesting that *Atp2c2* is a direct target of the MIST1 protein.

Discussion

MIST1 is a transcription factor required for complete acinar cell maturation and function. *Mist1*$^{-/-}$ acini display disrupted Ca^{2+} movement upon secretagogue stimulation, an altered exocytosis ability and increased sensitivity to caerulein-induced pancreatitis [5, 12] suggesting that *Mist1*$^{-/-}$ acinar cells have defects in the expression of Ca^{2+} handling proteins. However, to date no alterations in Ca^{2+}ATPase proteins have been documented in this model. In the current study, we identified a specific loss of the Ca^{2+}ATPase *Atp2c2*/SPCA2 in *Mist1*$^{-/-}$ pancreatic acinar cells as well as in other secretory cells that normally express MIST1, suggesting a link. While the loss of SPCA2 correlated with expansion of the Golgi compartment and disruption in protein glycosylation, the pancreatic isoform of SPCA2 does not localize to the Golgi, nor does it contain many of the domains required for Ca^{2+} pump action. Therefore, we have identified a novel isoform of the *Atp2c2* gene that may be, in part, responsible for the altered acinar cell phenotype observed in *Mist1*$^{-/-}$ mice.

Unlike past studies on Ca^{2+} ATPase expression, we observed increased accumulation of *Atp2a* (SERCA) and *Atp2b* (PMCA) pumps. There are two possibilities for the differences in expression. First, this study examines mRNA levels in vivo, while Luo et al (2005) examined protein levels in cultured acini. There may be differences in transcript or protein accumulation or the culturing of the cells could account for differences in expression. Second, the antibodies used by Luo et al (2005) were not specific to individual PMCA or SERCA isoforms. Since we have not performed an exhaustive study for all SERCA and PMCA isoforms, it is possible that the total levels are equal. In any event, the only *Atp2* gene that is reduced in *Mist1*$^{-/-}$ pancreatic tissue is *Atp2c2*. Mouse genetic studies showed that reactivation of MIST1 was closely followed by increased *Atp2c2* transcript levels suggesting that *Atp2c2* may be a downstream target of MIST1 transcriptional activity. Indeed, the overall expression pattern for *Atp2c2* correlated predominantly with MIST1 expression. Previous studies have revealed that *Atp2c2* is expressed in a number of tissues, most notably in the testes, brain and lactating mammary gland [20, 21]. While MIST1 is not found in testes or brain, it is expressed transiently in epithelial alveolar cells during lactation [20]. Similar to *Atp2c2*, expression of *Mist1* decreases to negligible levels upon mammary gland involution [22, 23]. Our studies have now extended the expression pattern of SPCA2 to include the secretory cells of pancreatic acini, salivary gland acini, seminal vesicles and stomach epithelium. In all cases, *Atp2c2*/SPCA2 expression correlates with MIST1 expression. Importantly, loss of MIST1 in these tissues produced dramatically decreased levels of *Atp2c2* and this expression pattern could be rescued in the pancreas within hours by inducing *Mist1*^{myc} transgene expression. Thus, although it remains possible that the absence of *Atp2c2*/SPCA2 reflects incomplete maturation of the *Mist1*$^{-/-}$ secretory cells and thus not a direct target of MIST1, given the rapid rescue response to MIST1^{myc} expression, this seems highly unlikely. Unfortunately, specific regulatory regions within the *Atp2c2* gene have not been identified so future studies employing MIST1 chromatin immunoprecipitation to show direct MIST1-promoter interactions will have to await further characterization the *Atp2c2* gene.

The full length SPCA2 is a Ca^{2+}ATPase that is thought to pump Ca^{2+} and Mn^{2+} from the cytosol into the Golgi where proper Ca^{2+} concentrations are required for accurate post-translational modifications [7]. The SPCA proteins are the mammalian equivalent to the PMR1 protein found in yeast and defective glycosylation and an altered secretory pathway are observed in *Pmr1*-deficient yeast, a phenotype similar to that found in *Mist1*$^{-/-}$ acini [24–26]. In addition, targeted ablation of the closely related mouse *Atp2c1* gene results in expansion of the Golgi compartment consistent with that observed in *Mist1*$^{-/-}$ acini [27]. It is interesting that a simlar phenotype is observed in *Mist1*$^{-/-}$ tissue without a decrease in *Atp2c1* expression levels.

While a model with MIST1 affecting exocrine cell function through the regulation of *Atp2c2* is attractive, we have uncovered novel findings regarding the structure and localization of the SPCA2 protein that adds considerable complexity. IF analysis indicated that SPCA2 does not co-localize with GM130 or adaptin γ at the Golgi apparatus. Instead, we show for the first time that SPCA2 localizes in the same location as the ER in both pancreas and salivary gland acinar cells. In agreement with our current observations, studies examining SPCA2 in neuronal cells also found that SPCA2 localizes to cellular regions outside of the Golgi apparatus [21]. Interestingly, localization of SPCA2 to the ER is more consistent with a role for this protein in regulated exocytosis. The Ca^{2+} required for exocytosis is contained within the ER of acinar cells, and during physiological stimulation, Ca^{2+} oscillations are observed within the apical portion of the acinar cells [28], suggesting that rapid release and uptake from the ER is essential for efficient transport of digestive enzymes out of the cell.

Even more intriguing is that our studies have uncovered a previously unknown pancreatic SPCA2 isoform that is significantly smaller (17–20 kDa) than the NCBI predicted SPCA2 protein (103 kDa). While it is possible that this protein represents a degradation product, our data support the existence of an alternative SPCA2 protein. First, immunoabsorption with the peptide used to generate the antibody eliminates the 20 kDa band observed in pancreatic protein extracts. Second, the 17–20 kDa SPCA2 band is detected in protein extracts from WT pancreata and in the acinar cell line AR42J. In contrast, no SPCA2 is detected in *Mist1*$^{-/-}$ samples or in the duct-like cell line ARIP. Finally, analysis of *Atp2c2* transcripts revealed a similar truncated mRNA only in WT RNA samples and not in *Mist1*$^{-/-}$ samples. The existence of different Ca^{2+}-ATPase isoforms is not unusual, as multiple isoforms exist for the SERCA, PMCA and SPCA1 pumps [17]. However, this particular isoform of *Atp2c2* is significantly different as it represents only the carboxy terminus of the protein. Based on RT-PCR and EST data, the pancreatic *Atp2c2* consists of at least the last six exons of the gene. This would include the 6th transmembrane domain and the carboxy domain for ion binding but exclude the Ca^{2+} transport site, phsophorylation sites, most transmembrane domains and the ATP binding site. Based on its structure, it is unlikely to act as an ion pump, sequester Ca^{2+} in the ER or even bind Ca^{2+} on its own.

We have attempted to identify the complete sequence of this novel *Atp2c2* transcript through 5′ RACE, degenerate primers, or mass spectrometry of protein extracts resolved by two-dimensional gel elctrophoresis. However, to date, most of our success stems from bioinformatic analysis of EST databases. ACEview suggests that 4 transcripts for *Atp2c2* exist, but none of these transcripts correlate to the size of mRNA observed in the pancreas. Based on ACEview, 75 ESTs exist with sequences identical to the *Atp2c2* gene. Eight of these ESTs were derived from pancreatic tissue, all aligned to the 3′ end of the gene. Not one of these ESTs would produce an alternative transcript that corresponds to the predicted molecular weight of the protein, which is in the range of 17 to 22 kDa. The largest pancreatic EST is AK007419, which was derived from a tiling array of cDNA from 10 day-old mouse pancreatic tissue. The EST is 704 bps and, when translated, produces a 104 amino acid protein that aligns with the carboxy terminus of the protein. All other pancreatic ESTs are less than 400 bp in length. There is a single EST identified that would produce a protein the size of the predicted pancreatic SPCA2 isoform. Accession #BI414588 was cloned from pooled lung tissue and is 935 bp long. It encodes exons 20–26 and translation from the first identified Kozak sequence would produce, in frame, a 185 amino acid protein. Further studies are necessary to determine if this represents the full length protein found in the pancreas.

In conclusion, we have identified a novel protein that is identical to the carboxy terminus of SPCA2. While lacking the functional domains required for Ca^{2+}-ATPase function, this

protein appears to accumulate in the ER, and is correlated to the expression of MIST1 in pancreatic acinar cells. Future work should focus on understanding how this alternative SPCA2 functions in the secretory pathway of MIST1-expressing cells and how MIST1 transcriptionally regulates *Atp2c2* gene expression.

Supplementary Material

Refer to Web version on PubMed Central for supplementary material.

Acknowledgments

Grant Support: This work was funded by operating grants from the Canadian Institutes of Health Research (MOP 53083), Children's Health Research Institute, and Lawson Health Research Institute to C.P. as well as by NIH DK55489 and NIH CA124586 to S.F.K. D.D. was supported by a Purdue Research Foundation Fellowship through the Purdue Center for Cancer Research. C.P. is supported by a salary award from the CIHR.

We would like to thank Drs. Gabriel DiMattia and Tom Drysdale and members of the Pin laboratory for the comments on suggestions on these studies, Dr. John Di Guglielmo for the kind gift of the GM130 antibody and to the Drysdale lab for their help and expertise with *in situ* hybridization.

Abbreviations

SPCA	secretory pathway Ca^{2+} ATPase
PMCA	plasma membrane Ca^{2+} ATPase
SERCA	sarcoendoplasmic reticulum Ca^{2+} ATPase
P-type	phosphorylation type
bHLH	basic helix-loop-helix
CCK	cholecystokinin
WT	wild type
ACC	acinar cell cultures
ER	endoplasmic reticulum

Reference List

1. Lemercier C, To RQ, Swanson BJ, Lyons GE, Konieczny SF. Mist1: a novel basic helix-loop-helix transcription factor exhibits a developmentally regulated expression pattern. Developmental biology. 1997; 182:101–113. [PubMed: 9073453]
2. Pin CL, Bonvissuto AC, Konieczny SF. Mist1 expression is a common link among serous exocrine cells exhibiting regulated exocytosis. The Anatomical record. 2000; 259:157–167. [PubMed: 10820318]
3. Cancela JM, Van Coppenolle F, Galione A, Tepikin AV, Petersen OH. Transformation of local Ca2+ spikes to global Ca2+ transients: the combinatorial roles of multiple Ca2+ releasing messengers. The EMBO journal. 2002; 21:909–919. [PubMed: 11867519]
4. Lee MG, Xu X, Zeng W, Diaz J, Kuo TH, Wuytack F, Racymaekers L, Muallem S. Polarized expression of Ca2+ pumps in pancreatic and salivary gland cells. Role in initiation and propagation of [Ca2+]i waves. The Journal of biological chemistry. 1997; 272:15771–15776. [PubMed: 9188473]
5. Luo X, Shin DM, Wang X, Konieczny SF, Muallem S. Aberrant localization of intracellular organelles, Ca2+ signaling, and exocytosis in Mist1 null mice. The Journal of biological chemistry. 2005; 280:12668–12675. [PubMed: 15665001]
6. MacLennan DH, Green NM. Structural biology. Pumping ions. Nature. 2000; 405:633–634. [PubMed: 10864310]

7. Wuytack F, Raeymaekers L, Missiaen L. PMR1/SPCA Ca2+ pumps and the role of the Golgi apparatus as a Ca2+ store. Pflugers Arch. 2003; 446:148–153. [PubMed: 12739151]
8. Cartwright EJ, Oceandy D, Neyses L. Plasma membrane calcium ATPase and its relationship to nitric oxide signaling in the heart. Annals of the New York Academy of Sciences. 2007; 1099:247–253. [PubMed: 17446465]
9. Missiaen L, Dode L, Vanoevelen J, Raeymaekers L, Wuytack F. Calcium in the Golgi apparatus. Cell calcium. 2007; 41:405–416. [PubMed: 17140658]
10. Pin CL, Rukstalis JM, Johnson C, Konieczny SF. The bHLH transcription factor Mist1 is required to maintain exocrine pancreas cell organization and acinar cell identity. The Journal of cell biology. 2001; 155:519–530. [PubMed: 11696558]
11. Shi G, Zhu L, Sun Y, Bettencourt R, Damsz B, Hruban RH, Konieczny SF. Loss of the acinar-restricted transcription factor Mist1 accelerates Kras-induced pancreatic intraepithelial neoplasia. Gastroenterology. 2009; 136:1368–1378. [PubMed: 19249398]
12. Kowalik AS, Johnson CL, Chadi SA, Weston JY, Fazio EN, Pin CL. Mice lacking the transcription factor Mist1 exhibit an altered stress response and increased sensitivity to caerulein-induced pancreatitis. American journal of physiology. 2007; 292:G1123–1132. [PubMed: 17170023]
13. Johnson CL, Weston JY, Chadi SA, Fazio EN, Huff MW, Kharitonenkov A, Koester A, Pin CL. Fibroblast growth factor 21 reduces the severity of cerulein-induced pancreatitis in mice. Gastroenterology. 2009; 137:1795–1804. [PubMed: 19664632]
14. Yule DI, Williams JA. U73122 inhibits Ca2+ oscillations in response to cholecystokinin and carbachol but not to JMV-180 in rat pancreatic acinar cells. The Journal of biological chemistry. 1992; 267:13830–13835. [PubMed: 1629184]
15. Johnson CL, Kowalik AS, Rajakumar N, Pin CL. Mist1 is necessary for the establishment of granule organization in serous exocrine cells of the gastrointestinal tract. Mechanisms of development. 2004; 121:261–272. [PubMed: 15003629]
16. Carafoli E, Genazzani A, Guerini D. Calcium controls the transcription of its own transporters and channels in developing neurons. Biochemical and biophysical research communications. 1999; 266:624–632. [PubMed: 10603299]
17. Zacharias DA, Strehler EE. Change in plasma membrane Ca2(+)-ATPase splice-variant expression in response to a rise in intracellular Ca2+ Curr Biol. 1996; 6:1642–1652. [PubMed: 8994829]
18. Vanoevelen J, Dode L, Van Baelen K, Fairclough RJ, Missiaen L, Raeymaekers L, Wuytack F. The secretory pathway Ca2+/Mn2+-ATPase 2 is a Golgi-localized pump with high affinity for Ca2+ ions. The Journal of biological chemistry. 2005; 280:22800–22808. [PubMed: 15831496]
19. Petersen OH, Burdakov D, Tepikin AV. Polarity in intracellular calcium signaling. Bioessays. 1999; 21:851–860. [PubMed: 10497335]
20. Anantamongkol U, Takemura H, Suthiphongchai T, Krishnamra N, Horio Y. Regulation of Ca2+ mobilization by prolactin in mammary gland cells: possible role of secretory pathway Ca2+-ATPase type 2. Biochemical and biophysical research communications. 2007; 352:537–542. [PubMed: 17129574]
21. Xiang M, Mohamalawari D, Rao R. A novel isoform of the secretory pathway Ca2+,Mn(2+)-ATPase, hSPCA2, has unusual properties and is expressed in the brain. The Journal of biological chemistry. 2005; 280:11608–11614. [PubMed: 15677451]
22. Reinhardt TA, Lippolis JD. Mammary gland involution is associated with rapid down regulation of major mammary Ca2+-ATPases. Biochemical and biophysical research communications. 2009; 378:99–102. [PubMed: 19000904]
23. Zhao Y, Johansson C, Tran T, Bettencourt R, Itahana Y, Desprez PY, Konieczny SF. Identification of a basic helix-loop-helix transcription factor expressed in mammary gland alveolar cells and required for maintenance of the differentiated state. Molecular endocrinology (Baltimore, Md. 2006; 20:2187–2198.
24. Durr G, Strayle J, Plemper R, Elbs S, Klee SK, Catty P, Wolf DH, Rudolph HK. The medial-Golgi ion pump Pmr1 supplies the yeast secretory pathway with Ca2+ and Mn2+ required for glycosylation, sorting, and endoplasmic reticulum-associated protein degradation. Molecular biology of the cell. 1998; 9:1149–1162. [PubMed: 9571246]

25. Rudolph HK, Antebi A, Fink GR, Buckley CM, Dorman TE, LeVitre J, Davidow LS, Mao JI, Moir DT. The yeast secretory pathway is perturbed by mutations in PMR1, a member of a Ca2+ ATPase family. Cell. 1989; 58:133–145. [PubMed: 2526682]

26. Antebi A, Fink GR. The yeast Ca(2+)-ATPase homologue, PMR1, is required for normal Golgi function and localizes in a novel Golgi-like distribution. Molecular biology of the cell. 1992; 3:633–654. [PubMed: 1379856]

27. Okunade GW, Miller ML, Azhar M, Andringa A, Sanford LP, Doetschman T, Prasad V, Shull GE. Loss of the Atp2c1 secretory pathway Ca(2+)-ATPase (SPCA1) in mice causes Golgi stress, apoptosis, and midgestational death in homozygous embryos and squamous cell tumors in adult heterozygotes. The Journal of biological chemistry. 2007; 282:26517–26527. [PubMed: 17597066]

28. Wasle B, Edwardson JM. The regulation of exocytosis in the pancreatic acinar cell. Cellular signalling. 2002; 14:191–197. [PubMed: 11812646]

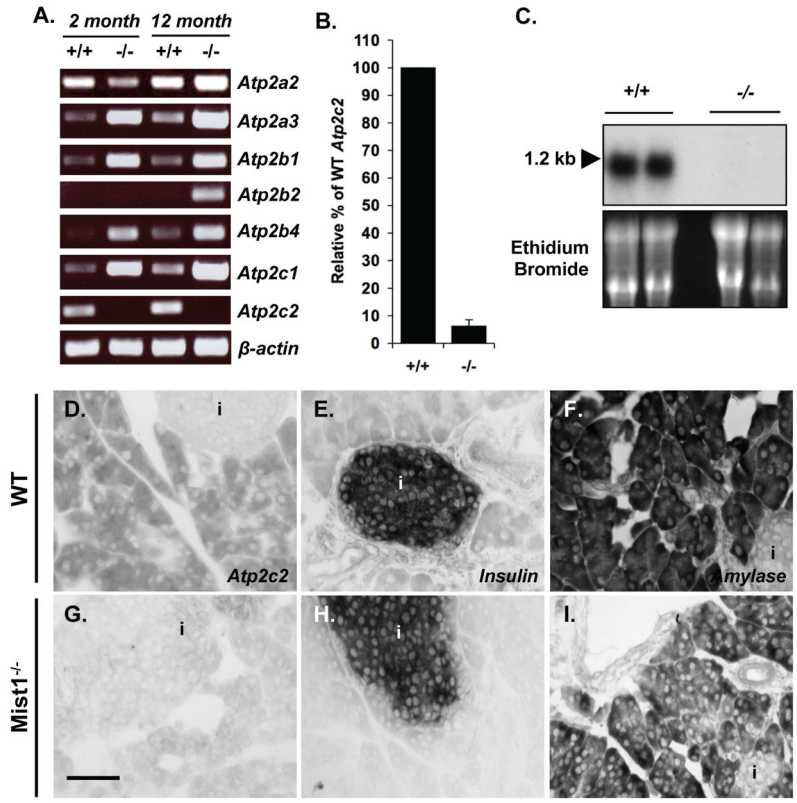

Figure 1. *Atp2c2* mRNA is reduced in *Mist1*$^{-/-}$ pancreatic tissue

(A) RT-PCR for *Atp2a2* and *3, Atp2b1, 2* and *4*, or *Atp2c1* and *2* on two and twelve month-old WT (+/+) and *Mist1*$^{-/-}$ (−/−) pancreatic RNA. β-*actin* was used as a positive control for RT reactions. **(B)** Quantitative RT-PCR for *Atp2c2* expression in WT and *Mist1*$^{-/-}$ pancreatic RNA. The WT amount is set to 100%. **(C)** Northern blot analysis on WT and *Mist1*$^{-/-}$ pancreatic RNA using a probe specific to the 3′ end of the *Atp2c2* sequence. **(D–I)** *In situ* hybridization on WT (**D–F**) and *Mist1*$^{-/-}$ **(G–I)** pancreatic tissue sections using probes for the 3′ end of *Atp2c2* (**D, G**), insulin (**E, H**) and amylase (**F, I**). Scale bar = 95 μm; i - islet.

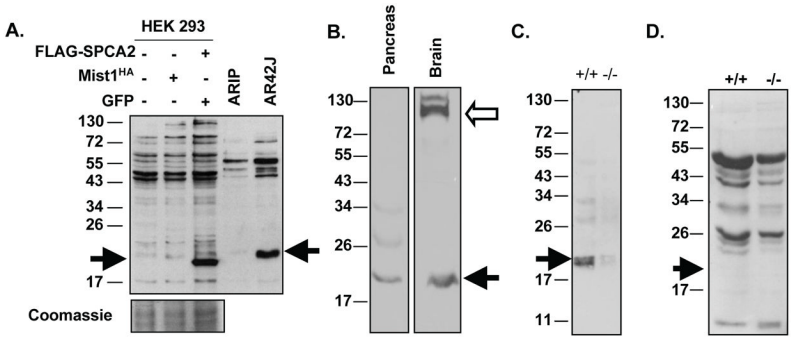

Figure 2. A truncated isoform of SPCA2/*Atp2c2* is expressed in pancreatic acinar cells

(A) Western blot for SPCA2 on protein extracts from HEK 293T cells transfected with *pcDNA3.0-FLAG-SPCA2*$^{760\text{-}944}$, *pcDNA3-Mist1*^{HA} or *pcDNA3-GFP* or from AR42J and ARIP cells. Coomassie staining was used to verify equal loading. A protein between 17–26 kDa (arrow) was identified in AR42J cells and not in ARIP cells. FLAG-SPCA2$^{760\text{-}944}$ produces a protein of approximately 20 kDa. **(B)** Western blot analysis on pancreatic and brain protein extracts identified the lower molecular weight isoform in both tissues (arrow) and the larger SPCA2 isoform only in the brain (open arrow). **(C)** Western blot analysis for SPCA2 reveals this smaller isoform only in WT (arrow) but not *Mist1*$^{-/-}$ pancreata. **(D)** Preabsorption with a SPCA2 blocking peptide completely abolished detection of the protein. Higher molecular weight bands begin to appear at longer exposures of the blots.

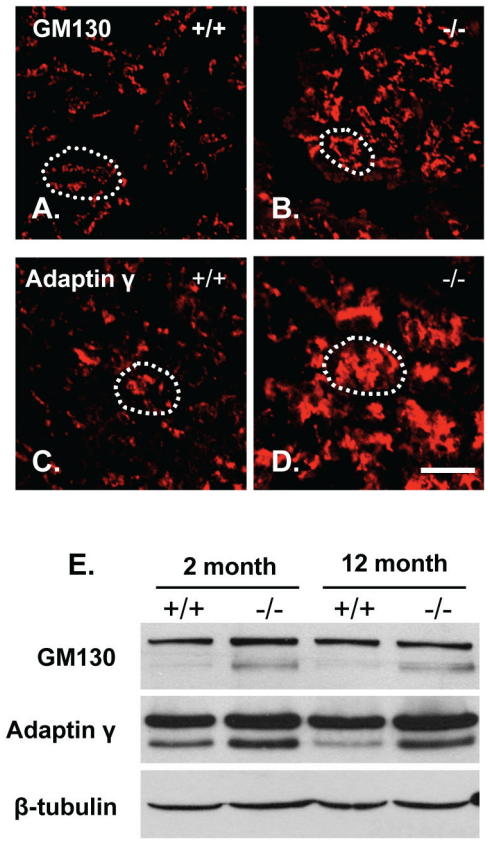

Figure 3. ***Mist1*** $^{-/-}$ **acinar cells have an expanded Golgi apparatus**

(A–D) IF on pancreatic sections for Golgi-specific markers GM130 **(A, B)** or adaptin γ **(C, D)**. White dotted lines indicate an acinus. Scale bars = 40 μm. **(E)** Western blot analysis for GM130 and adaptin γ on 2 and 12 month WT (+/+) and ***Mist1*** $^{-/-}$ (−/−) pancreatic protein. β-tubulin was used as a loading control.

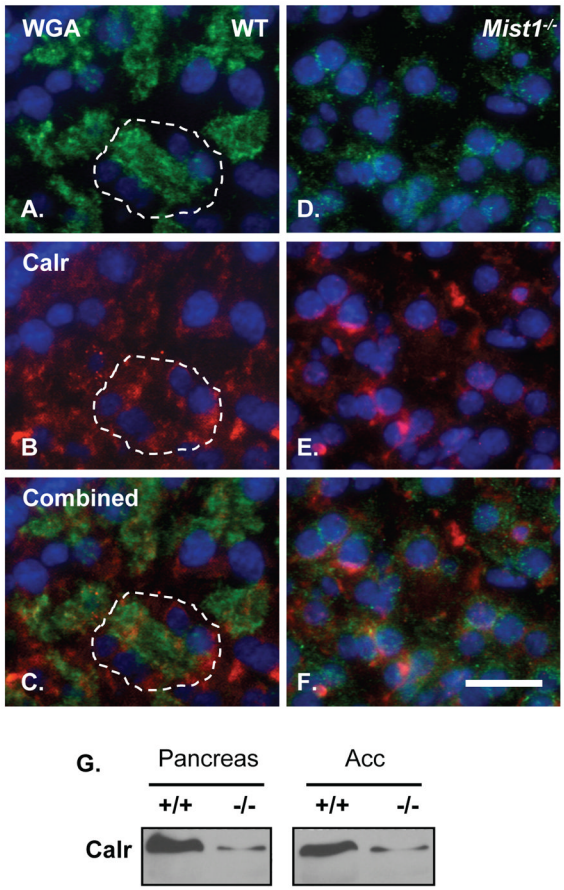

Figure 4. Altered cellular function in *Mist1*$^{-/-}$ acini

Localization of FITC-WGA (**A, D**) combined with IF analysis for calreticulin (Calr; **B, E**) in WT (**A–C**) and *Mist1*$^{-/-}$ (**D–F**) pancreatic acini. Images were merged in panels **C** and **F**. DAPI was used to stain the nuclei (blue). An acinus is indicated in WT sections by the white dashed lines. Scale bars = 20 μm. **(G)** Western blot analysis for Calreticulin (Calr) in WT (+/+) and *Mist1*$^{-/-}$ (−/−) pancreata or purified acinar cell (Acc) extracts.

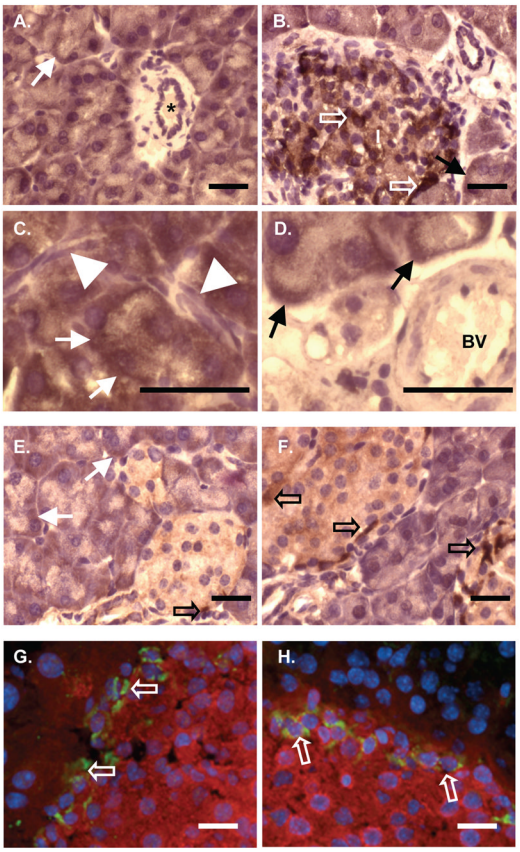

Figure 5. SPCA2 is expressed in acinar cells and a subset of islet cells in the pancreas

(A–F) IHC for SPCA2 on pancreatic tissue shows expression in acinar cells (arrows) and a subset of islet (I) cells (open arrows, **B**), but not in ducts (*, **A**), intercalated duct (arrowheads, **C**) or blood vessels (BV, **D**). IHC for SPCA2 or co-IF **(G, H)** for SPCA2 (green) and insulin (red) in wild type **(E, G)** and *Mist1*$^{-/-}$ **(F, H)** tissue reveals maintenance of SPCA2 in the islets even after deletion of *Mist1*. Magnification bars = 20 μm.

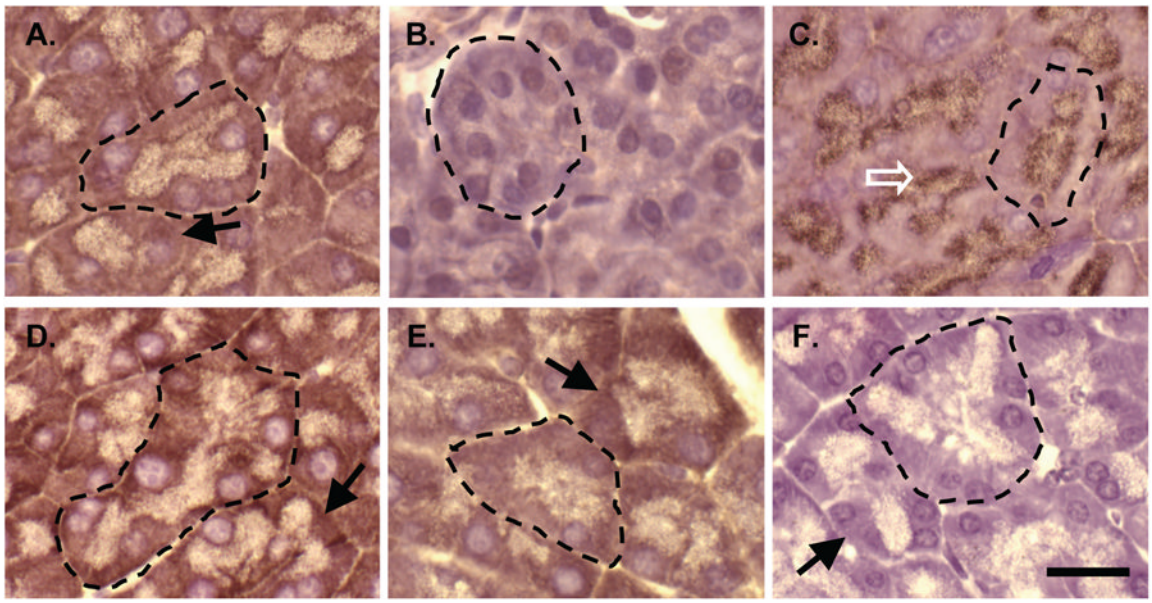

Figure 6. SPCA2 is localized to the basal aspect of acinar cells typical of ER localization

IHC for SPCA2 on wild type (**A**) or *Mist1*$^{-/-}$ (**B**) pancreatic tissue, or for adaptin γ (**C**), calreticulin (**D**), SERCA2 (**E**) or with no primary antibody (**F**). Individual acini have been outlined with a dotted line and staining consistent with the ER (arrows) or Golgi apparatus (open arrow) indicated in an adjacent acinus. Magnification bar = 20 μm.

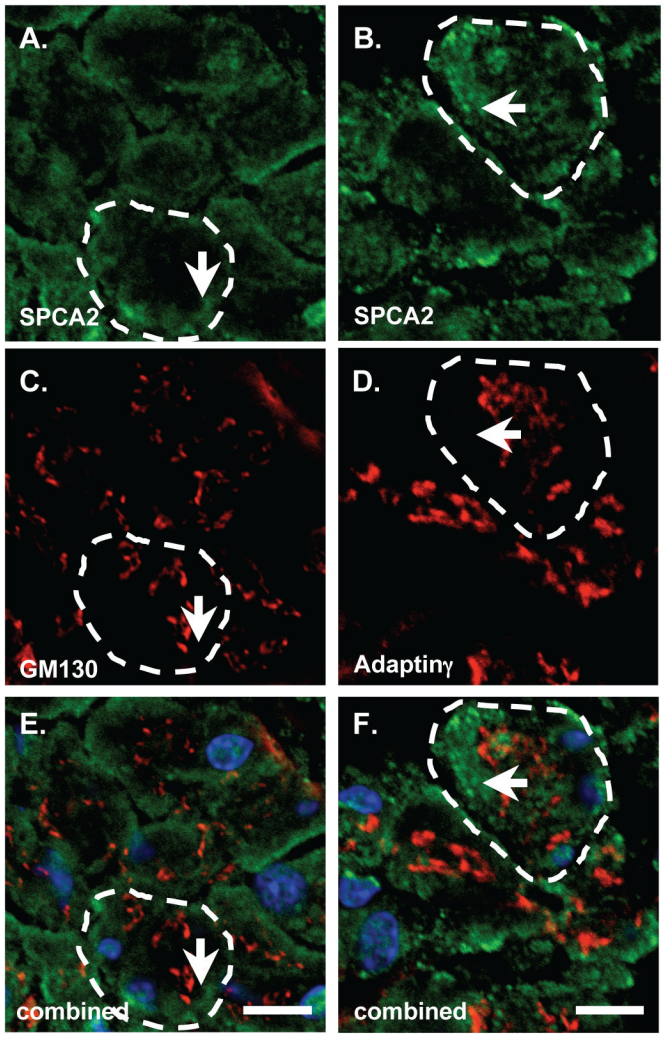

Figure 7. SPCA2 is not localized to the Golgi apparatus in pancreatic acinar cells

Confocal co-IF on pancreatic sections for Golgi-specific markers, GM130 **(C)** or adaptin γ **(D)** and SPCA2 **(A, B)**. White dotted lines indicate a single acinus. Scale bars = 10 μm. DAPI was used to stain the nuclei (blue). **(E, F)** Represent the merged images of SPCA2 and the Golgi markers.

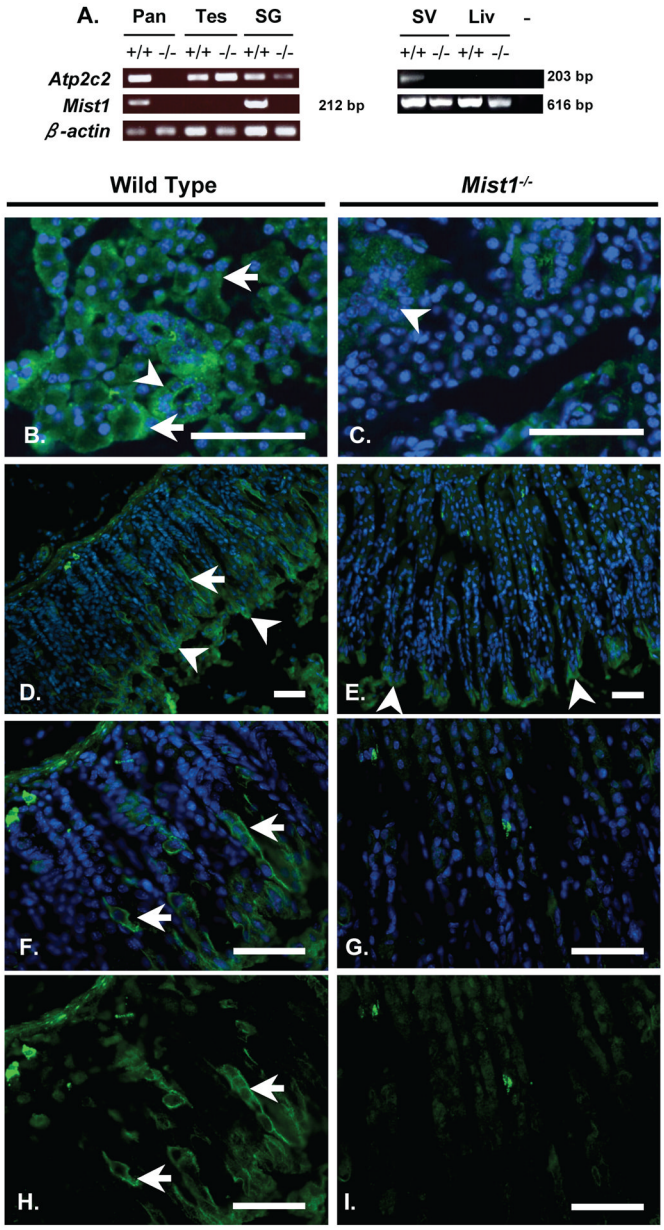

Figure 8. *Atp2c2*/SPCA2 accumulation is reduced in other MIST1-expressing tissue in *Mist1*$^{-/-}$ mice

(A) RT-PCR for *Atp2c2*, *Mist1* or *β-actin* in RNA extracts from pancreas (Pan), testes (Tes), salivary glands (SG), seminal vesicle (SV) and liver (Liv). No RT (−) was added to the negative control. **(B–I)** IF for SPCA2 on salivary glands **(B, C)** and stomach **(D–I)** sections from WT (**B, D, F, H**) and *Mist1*$^{-/-}$ (**C, E, G, I**) mice. Arrows in **B** indicates basal localization of SPCA2 in salivary gland acini. Arrowheads in **B** and **C** indicate SPCA2 expression in duct cells of the salivary gland, which are not positive for MIST1. Arrowheads in **D** and **E** indicate SPCA2+ cells at the surface of epithelial crypts in both strains of mice while arrows indicate SPCA2 positive cells with the epithelial crypts only in WT stomach sections. Images **F–I** are higher magnifications of **D** and **E** to better reveal SPCA2+ cells. All panels identify nuclei through DAPI staining expect **H** and **I**. Scale bar = 50 μM.

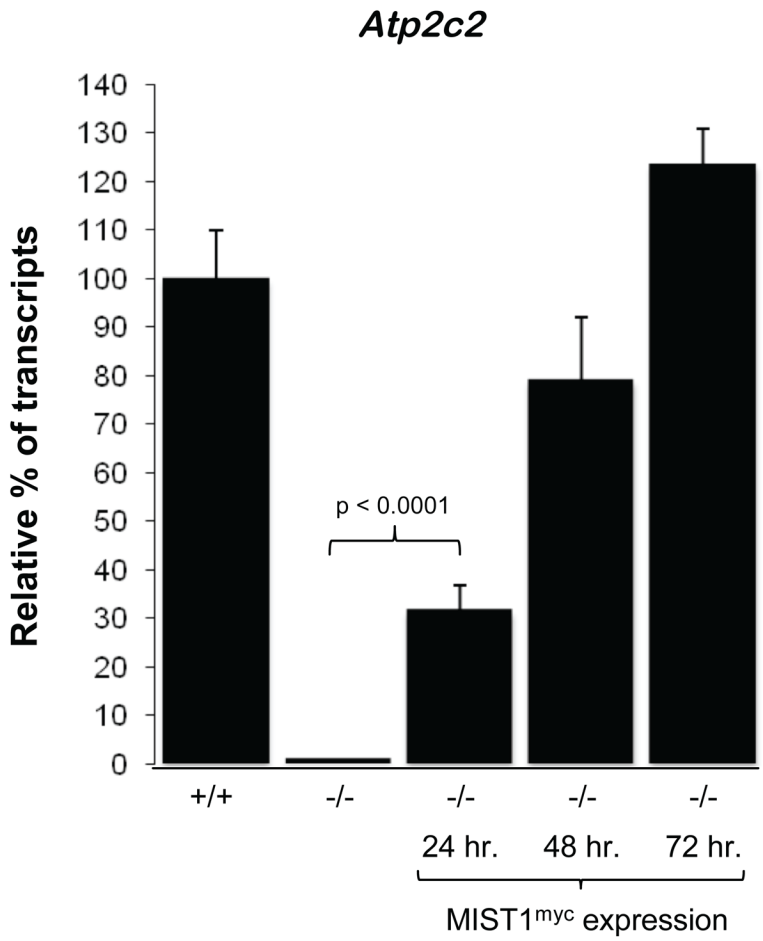

Figure 9. MIST1 re-expression rescues *Atp2c2* expression

Quantitative RT-PCR for *Atp2c2* following a single dose of tamoxifen in *Mist1*$^{CreER/CreER}$/*LSL-Mist1*^{myc} mice. WT levels are set at 100% and compared to wild type (+/+), *Mist1*$^{-/-}$ (−/−) or 24, 48 or 72 hours after induction of MIST1^{myc} expression. Error bars represent mean ± SE; n=3.